

Parallel Algorithm for Collision Avoidance Motion Planning of Dual Arm Grasping of Humanoid Robot

Hua-Zhong Li, Yong-Sheng Liang**, Qiang-ping Tang

Shenzhen Institute of Information Technology, Shenzhen, 518172, China

Received 12 September 2014, www.cmmt.lv

Abstract

Aiming at such problems as grasping space limitation, unknown target configuration, DOF redundancy of dual arm and singular configuration for collision avoidance motion planning of simultaneous grasping of high-dimensional space humanoid robot, firstly, forward kinematics for dual arm of humanoid robot and SVD-based inverse kinematics models have been established. Secondly, this paper has put forward a parallel algorithm for dual arm grasping motion planning framework integrating SVD and RRT techniques and DAGRRT collision avoidance motion planning. Finally, the correctness and effectiveness of the algorithm proposed in this paper has been verified via computer 3D visualization simulation.

Keywords: humanoid robot, dual arm grasping, rapidly-exploring random tree (RRT), singular value decomposition (SVD), DAGRRT planner, parallel algorithms.

1 Introduction

The collision avoidance motion planning of complex space object grasped by dual arm of humanoid robot is a typical high-dimensional C-space and nonlinear constrained motion planning issue as well as a challenging frontier research field [1-4]. It is becoming a research focus for scholars at home and abroad [5-10].

At present, the motion planning of high-dimensional space robot mainly includes two kinds of typical random sampling methods: Probabilistic Road Map (PRM) [11-15] and Rapidly-exploring Random Tree (RRT) [16-21].

Kuffner and Wang Wei et al succeeded in applying RRT method in bipedal robot H5 to solve such motion planning problems as walking, gesture conversion, single arm grasping and control [22-24]. As for the structure of joint-type humanoid robot lacking the analytical solution for inverse kinematics, these literatures provide the heuristic information mainly according to the robot's configuration state in the work space end effector, adopt the RRT motion planning method based on random sampling theory and provide new solution ideas for the motion planning of humanoid robot. Bertram et al utilized the distance measurement for the end effector of humanoid robot in work space opposite to the object configuration as the heuristic information for C-space motion planning, and led RRT algorithm to rapid expansion of target configuration [25]. Weghe et al utilized Jacobi matrix transposition method to directly translate the heuristic information in work space into joint space configuration, which has improved the performance of motion planning algorithm of humanoid robot [26]. Berenson et al utilized the projection technology to put forward limited two-way RRT algorithm, move the sampling road points in C-space to the constraint manifold and realize the rapid motion planning of single arm grasping of mechanical arm with 7 DoFs [27-29].

Aiming at the collision avoidance motion planning of dual arm grasping of humanoid robot, this paper firstly

studies the modelling methods for forward kinematics and inverse kinematics of dual arm. Secondly, it has put forward the framework model for collision avoidance motion planning of dual arm grasping based on RRT as well as a parallel processing algorithm for DAGRRT collision avoidance motion planning integrating SVD and RRT techniques. Finally, the correctness and effectiveness of the algorithm proposed in this paper has been verified via computer 3D visualization simulation.

2 Model For Dual Arm Kinematics

2.1 FORWARD KINEMATICS

Refer to Fig.1 for schematic diagram for dual arm model of humanoid robot studied in this paper. Left (right) arm has 7 rotational DOFs, and D-H method is adopted to describe each rotational joint parameter $(q_i^k, \alpha_i^k, a_i^k, d_i^k)$. Each coordinate system is recorded as ${}^k\Sigma_i({}^kx_i, {}^ky_i, {}^kz_i)$, and each joint angle as q_i^k and arm configuration as $\mathbf{q}^k = [q_0^k, \dots, q_6^k]^T$ (k=R, L refer to left/right arm; i=0~6 refer to 7 rotating joints including shoulder 1, shoulder 2, upper arm, elbow, forearm, wrist 1 and wrist 2). If $\sin q_i^k$ and $\cos q_i^k$ are simplified as $s_{q_i^k}$ and $c_{q_i^k}$, the homogeneous transformation matrix ${}^k\mathbf{T}_{i+1}^i(q_i^k)$ between the coordinate systems ${}^k\Sigma_{i+1}$ and ${}^k\Sigma_i$ can be expressed as Formula (1):

* Corresponding author e-mail: liangys@sziit.edu.cn

$${}^k T_{i+1}^i(q_i^k) = \begin{bmatrix} c_{q_i^k} & -c_{\alpha_i^k} s_{q_i^k} & s_{\alpha_i^k} s_{q_i^k} & a_i^k c_{q_i^k} \\ s_{q_i^k} & c_{\alpha_i^k} c_{q_i^k} & s_{\alpha_i^k} c_{q_i^k} & a_i^k s_{q_i^k} \\ 0 & s_{\alpha_i^k} & c_{\alpha_i^k} & d_i^k \\ 0 & 0 & 0 & 1 \end{bmatrix} \quad (1)$$

$$\mathbf{R} = \begin{bmatrix} c_\phi c_\theta c_\psi - s_\phi s_\psi & -c_\phi c_\theta s_\psi - s_\phi c_\psi & c_\phi s_\theta \\ s_\phi c_\theta c_\psi + c_\phi s_\psi & -s_\phi c_\theta s_\psi + c_\phi c_\psi & s_\phi s_\theta \\ -s_\theta c_\phi & s_\theta s_\psi & c_\theta \end{bmatrix}. \quad (4)$$

If the rotation matrix \mathbf{R} is known, the Euler angle can be calculated according to Formula (5):

$$\begin{cases} \phi = a \tan 2(a_y, a_x) \\ \theta = a \tan 2(c_\phi a_x + s_\phi a_y, a_z) \\ \psi = a \tan 2(s_\phi n_x + c_\phi n_y, s_\phi s_x + c_\phi s_y) \end{cases}. \quad (5)$$

Considering that inverse cosine function cannot determine the characteristic of plus-minus sign of the angle, arc-tan function $\text{atan2}(y, x)$ is adopted in this paper to determine the Euler angle within $[-\pi, \pi]$.

2.2 FORWARD KINEMATICS

The time t is derived from Formula (3), and then the differential relation (6) between dual arm configuration \mathbf{q}^k and configuration \mathbf{x}^k of dual arm of humanoid robot:

$$\dot{\mathbf{x}}^k = \mathbf{J}_k(\mathbf{q}^k) \dot{\mathbf{q}}^k, \quad (6)$$

Where, $\dot{\mathbf{x}}^k$ is the generalized velocity of the end of dual arm of humanoid robot in operating space, $\dot{\mathbf{q}}^k$ is the joint speed, and $\mathbf{J}_k(\mathbf{q}^k)$ is the partial derivative matrix of 6×7 . That is, it is Jacobi matrix of dual arm, and the elements in No. i line and No. j row are:

$$J_{ij}^k(\mathbf{q}^k) = \frac{\partial f_i^k(\mathbf{q}^k)}{\partial q_j^k} \quad (i=0, \dots, 5 \quad j=0, \dots, 6). \quad (7)$$

In the base coordinate system Σ_0 , Jacobi matrix $\mathbf{J}_k(\mathbf{q}^k) \in R^{6 \times 7}$ of dual arm of humanoid robot can be expressed as Formula (8):

$$\mathbf{J}_k(\mathbf{q}^k) = [J_1^k(q_0^k) \quad \dots \quad J_1^k(q_6^k)], \quad (8)$$

Wherein, $J_1^k(q_0^k) = \begin{bmatrix} z_i^k \times {}^i p_n^k \\ z_i^k \end{bmatrix}$, z_i^k and ${}^i p_n^k$ are the

expressions in the base coordinate system Σ_0 , and \times refers to vector product. Use singular value decomposition (SVD), $\mathbf{J}_k(\mathbf{q}^k)$ can be expressed as Formula (9):

$$\mathbf{J}_k(\mathbf{q}^k) = \mathbf{U}_k \mathbf{D}_k \mathbf{V}_k^T, \quad (9)$$

Wherein, $\mathbf{U}_k \in R^{6 \times 6}$ and $\mathbf{V}_k \in R^{7 \times 7}$ are orthogonal matrixes, $\mathbf{D}_k \in R^{6 \times 7}$. Thus, the generalized inverse matrix $\mathbf{J}_k^+(\mathbf{q}^k)$ can be written as the vector form in Formula (10):

$$\mathbf{J}_k^+(\mathbf{q}^k) = \sum_{i=1}^r \sigma_i^{-1} v_i u_i^T, \quad (10)$$

Wherein, $\sigma_i = d_{i,i}$ is $\mathbf{J}_k(\mathbf{q}^k)$ eigenvalue of $\mathbf{J}_k(\mathbf{q}^k)$, r is the sequence of $\mathbf{J}_k(\mathbf{q}^k)$. u_i and v_i refer to No. i row of \mathbf{U}_k and \mathbf{V}_k respectively.

Therefore, according to Formula (6), the differential form for inverse kinematics of dual arm of humanoid robot based on SVD can be written as Formula (11):

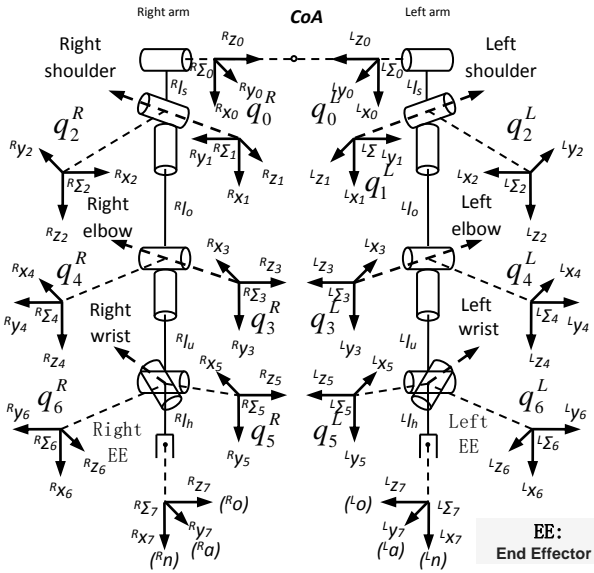


Figure 1 Schematic diagram for dual arm of humanoid robot

When taking dual arm centre (CoA) as an original point of the reference coordinate system Σ_0 , the matrix form of forward kinematical equation for dual arm can be expressed as Formula (2):

$${}^k T_7^0(\mathbf{q}^k) = \prod_{i=0}^7 {}^k T_{i+1}^i(q_i^k) = \mathbf{T}_{tcp}^k, \quad (2)$$

Wherein, $\mathbf{T}_{tcp}^k = \begin{bmatrix} \mathbf{n}^k & \mathbf{o}^k & \mathbf{a}^k & \mathbf{p}^k \\ 0 & 0 & 0 & 1 \end{bmatrix}$ refers to

homogeneous matrix of TCP configuration of humanoid robot, \mathbf{n}^k , \mathbf{s}^k , \mathbf{a}^k and \mathbf{p}^k refer to normal vector, sliding vector, approach vector and position vector of left (right) arm. Formula (2) can be converted into the classic vector form expressed in Formula (3):

$$\mathbf{x}^k = \mathbf{f}^k(\mathbf{q}^k), \quad (3)$$

Wherein, $\mathbf{q}^k \in R^7$ refers to configuration vector of left (right) arm of humanoid robot, $\mathbf{x}^k [x, y, z, \phi, \theta, \psi] \in R^6$ refers to TCP configuration vector at the end of left (right) arm, including 3D position vector (x, y, z) and 3D Euler angle (ϕ, θ, ψ) configuration vector. The configurations expressed by Euler angle and the configuration described by rotation matrix $\mathbf{R} = [\mathbf{n} \quad \mathbf{o} \quad \mathbf{a}]$ have the following transformational relation. If the Euler angle is known, the rotation matrix \mathbf{R} (4) can be inferred according to $\mathbf{R} = \mathbf{R}_{z,\phi} \mathbf{R}_{y,\theta} \mathbf{R}_{z,\psi}$:

$$\dot{\mathbf{q}}^k = \mathbf{J}_k^+(\mathbf{q}^k)\dot{\mathbf{x}}^k \quad (11)$$

To facilitate the numerical calculation, the increment equation for inverse in Formula (11) can be expressed as Formula (12):

$$\Delta\mathbf{q}^k = \mathbf{J}_k^+(\mathbf{q}^k)\Delta\mathbf{x}^k \quad (12)$$

3 DAGRRT algorithm

Refer to Fig.2 for simultaneous grasping of 3D space object by the dual arm of humanoid robot integrating RRT and SVD techniques and the framework of collision avoidance motion planner DAGRRT (Dual-Arm Grasping RRT). Refer to Algorithm 1 for its core pseudo-code realization. DAPGT: DArms Parallel Grasp Trajectory; SAGT:Single Arm Grasp Trajectory.

Algorithm 1: DAGRRT($\mathbf{q}_s^L, \mathbf{q}_s^R, \mathbf{x}_{obj}$) {

```

01  $RRT^L = GRRT(\mathbf{q}_s^L, \mathbf{x}_{obj})$ ;// construct grasping object of left arm
02  $RRT^R = GRRT(\mathbf{q}_s^R, \mathbf{x}_{obj})$ ;//construct grasping object of right arm
03  $RRT^L.start(); RRT^R.start()$ ;//start planning process of left and right arms
04 do {
05#pragma omp parallel // OpenMP parallelization of left arm algorithm.
06  $s^L = RRT^L.getNewPath()$ ;//process the outcome of left arm planning
07 if(  $s^L$  ) { //if the path is non-void
08      $S^L.add(s^L)$ ; add it to the outcome set of left arm planning
09     foreach(  $s^R \in S^R$  ) { //traverse the outcome set of right arm planning
10         //if meeting grasping quality criteria and collision avoidance requirements
11         if(GraspScore( $s^L, s^R$ ) >  $gs_{min}$ )&&
12             !Collision( $s^L, s^R$ ) ) { StopLoop=true;
13     } }
14#pragma omp parallel // OpenMP parallelization of right arm algorithm.
15  $s^R = RRT^R.getNewPath()$ ;//process the outcome of right arm planning
16 if(  $s^R$  ) { //if the path is non-void
17      $S^R.add(s^R)$  add it to the outcome set of left arm planning
18     foreach(  $s^L \in S^L$  ) { // traverse the outcome set of left arm planning
19         if(GraspScore( $s^L, s^R$ ) >  $gs_{min}$ )&&
20             !Collision( $s^L, s^R$ ) ) { StopLoop=true;
21     } }
22 }while(!StopLoop);
23#pragma omp critical //the main thread waits for the completion of other paralleled tasks
24  $RRT^L.stop(); RRT^R.stop()$ ;//stop the planning process

```

of left and right arms
 25 return CreatePath(s^L, s^R); }

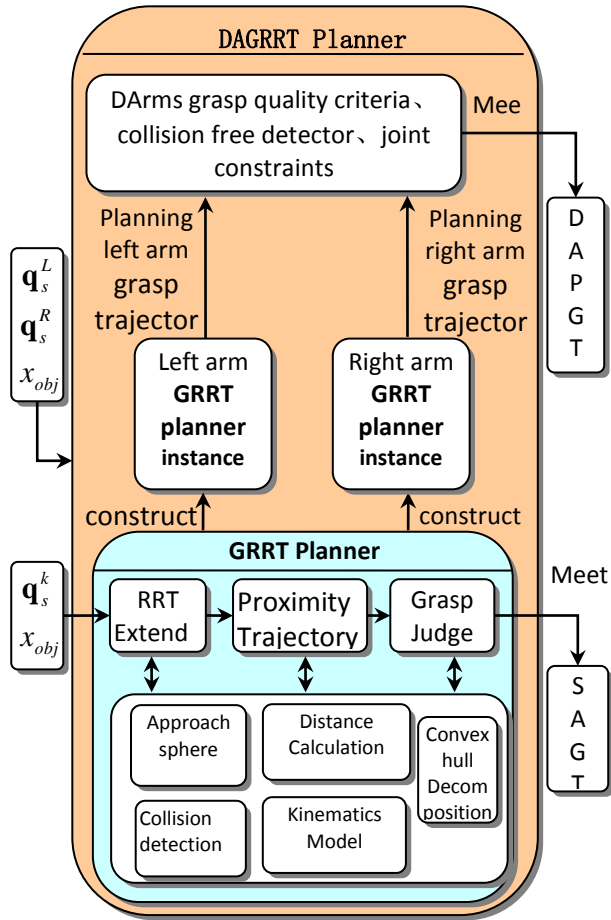


FIGURE 2 DAGRRT planner framework

Explanation for Algorithm 1: To realize the parallel planning of dual arm grasping, left (right) arm grasping planner $GRRT(\mathbf{q}_s^k, \mathbf{x}_{obj})$ adopts independent thread realization ($k=R, L$ refer to left and right arms), and the superscript L(\$\$) is marked as relevant planning parameters of left (right) arms. Multi-core technology based on OpenMP is used to realize the parallelization processing for the algorithm so as to accelerate the planning. Parameter gs_{min} is the minimum evaluation index to judge the effectiveness of object grasped by dual arm. C_{grasp}^L and C_{grasp}^R refer to the contact point sets for left and right hands. According to the hand grasping force closing principle obtained from the analysis of grasping wrench space (GWS), the union set $C_{grasp} = C_{grasp}^L \cup C_{grasp}^R$ can be used to adjust contact force, construct the convex hull, which is similar to single hand and then realize the pseudo-code of GraspScore (s^L, s^R), as shown in Algorithm 2 ($n_{contact}^L$ and $n_{contact}^R$ refer to the minimum finger quantity for left and right hands to contact with the objects.). Collision (s^L, s^R) is realized by adopting HBV (Hierarchical Bounding Volume) algorithm for directions, and its basic idea is as follows: A big solid bounding volume is used to

substitute the geometrical model of complex objects. By intersection test among bounding volumes, the non-intersection basic geometrical element pairs can be quickly eliminated so as to reduce the workload of intersection test. To realize the collision detection precision, the hierarchical method should be firstly adopted to establish HBV and approach to the complex geometrical model until all characteristics of the model can be completely described, and then separating axis theory can be used to conduct dual traversal test among bounding box trees so as to judge whether there is any collision [30-34].

Algorithm 2: GraspScore(s, s^R) {

```
01  $C_{grasp}^L = \text{GetContactPoints}(s^L)$ ; //calculate the contact
point set for left hand
02  $C_{grasp}^R = \text{GetContactPoints}(s^R)$ ; //calculate the contact
point set for right hand
03 if ( $|C_{grasp}^L| < n_{contact}^L \parallel |C_{grasp}^R| < n_{contact}^R$ ) return 0;
04  $C_{grasp} = C_{grasp}^L \cup C_{grasp}^R$ ;
05 return GraspQualityMeasure( $C_{grasp}$ ); }
```

Refer to Algorithm for pseudo-code realization of left (right) arm grasping planner GRRT algorithm.

Algorithm 3: GRRT($\mathbf{q}_s^k, \mathbf{x}_{obj}$) {

```
01  $RRT^k$ .initConfig( $\mathbf{q}_s^k$ ); //set initial configuration of RRT
tree
02 StopLoop=false; // set stop loop mark
03 do {
04  $f_r = \text{rand}() * (1.0 / (0x7fff))$ ; // generate random sampling
probability between (0, 1)
05 if ( $f_r \leq f \text{ ConnectJacobian}$ ) { // execute routine
extend/connect
06 ExtGraspStatus =  $RRT^k$ .ApproachToTarget( $\mathbf{x}_{obj}$ );
07 switch (ExtGraspStatus) {
08 case FatalError: StopSearch=true; break; //fatal error
09 case TargetReached: //reach target grasping configuration
10 if (Grasps.size() <= 0) StopSearch=true; //stop searching
11 else { FoundSolution=true; //find search solution
12 graspInfo = Grasps[Grasps.size()-1];
13  $\mathbf{q}_g^k = \text{getTargetConfig}(\text{graspInfo.nRrtNodeId})$ ;
14 break; //obtain the target configuration
15 } else { //Expand to C-space random configuration
16  $RRT^k$ .getRandConfig( $\mathbf{q}_r^k$ ); //obtain C-space random
configuration
17  $\mathbf{q}_n^k = RRT^k$ .NNConfig( $\mathbf{q}_r^k$ ); //search RRT nearest
configuration
18 ExtStatus =  $RRT^k$ .Connect( $\mathbf{q}_n^k, \mathbf{q}_r^k, \mathbf{q}_{new}^k$ );
19  $RRT^k$ .addConfig( $\mathbf{q}_{new}^k$ ); //add new configuration to
RRT tree
20 if (ExtendStatus==ERROR) StopSearch=true;
21 }
```

```
22 Cycles++; //add 1 to search times
23 if (StopSearch || FoundSolution || (Cycles > MaxCycles))
24 StopLoop=true; //set stop loop mark
25 } while (!StopLoop);
26 getNewPath( $\mathbf{q}_s^k, \mathbf{q}_g^k$ ); }
```

Explanation for Algorithm 3: Set f ConnectJacobian as 0.3, the maximum cycle search times are MaxCycles = 40,000. getRandConfig(\mathbf{q}_r^k) are evenly distributed in left (right) C-space. After random sampling, the random configuration $\mathbf{q}_r^k = \mathbf{q}_{min}^k + \text{rand}() * (1 / 0x7fff) * (\mathbf{q}_{max}^k - \mathbf{q}_{min}^k)$ can be obtained. NNConfig(\mathbf{q}_r^k) seeks the configuration \mathbf{q}_n^k , which is nearest to \mathbf{q}_r^k in left (right) arm rapidly-exploring random tree RRT^k . That is, $\min \|\mathbf{q}_n^k - \mathbf{q}_r^k\|^2 = \min \sum_{i=0}^6 (q_{n,i}^k - q_{r,i}^k)^2$. Connect($\mathbf{q}_n^k, \mathbf{q}_r^k, \mathbf{q}_{new}^k$) realizes the expansion for left (right) arms of humanoid robot from the nearest configuration \mathbf{q}_n^k to the random configuration \mathbf{q}_r^k until the obstacle is met. A new configuration \mathbf{q}_{new}^k is obtained and added to RRT^k . Its schematic diagram for operating principle is shown in Figure 3.

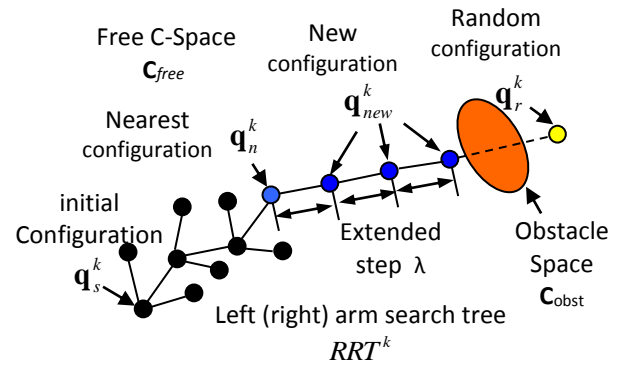


FIGURE 3 Operating principle of Connect($\mathbf{q}_n^k, \mathbf{q}_r^k, \mathbf{q}_{new}^k$)

ApproachToTarget(\mathbf{x}_{obj}) is to adopt the core algorithm, in which SVD generalized inverse kinematics expands to the target configuration. Its pseudo-code realization is shown in Algorithm 4.

Algorithm 4: ApproachToTarget(\mathbf{x}_{obj}) {

```
01 calculateGlobalGraspPose(grasp); //calculate global
grasping object
02  $\mathbf{x}_{target}^k = \text{ComputeTargetPose}(\text{grasp}, \mathbf{x}_{obj})$ ; //target
configuration
03  $\mathbf{q}_{near}^k = RRT^k$ .GetNearestNeighbor( $\mathbf{x}_{target}^k$ );
04 do {
05  $\mathbf{x}_{near}^k = FK^k(\mathbf{q}_{near}^k)$ ; //forward kinematics of left (right)
arms as per Formula (3)
06  $\Delta \mathbf{x}^k = \mathbf{x}_{target}^k - \mathbf{x}_{near}^k$ ; //calculate Cartesian space
configuration difference
```

```

07  $\Delta \mathbf{x}_{step}^k = \text{LimitStepSize}(\Delta \mathbf{x}^k)$ ; // calculate configuration
increment
08  $\Delta \mathbf{q}^k = \mathbf{J}_k^+(\mathbf{q}_{near}^k) * \Delta \mathbf{x}^k$ ; // obtain configuration increment
as per Formula (12)
09  $\mathbf{q}_{near}^k += \Delta \mathbf{q}^k$ ; // calculate the new configuration after
artificial arm moves the little configuration
10 if (Collision( $\mathbf{q}_{near}^k$ ) || !InJointLimits( $\mathbf{q}_{near}^k$ ))
11     return FatalError;
12  $RRT^k.AddConfig(\mathbf{q}_{near}^k)$ ;
13 } while ( $\|\Delta \mathbf{x}^k\| \geq \|\Delta \mathbf{x}_{Threshold}^k\|$ );
14 return TargetReached; }
    
```

Algorithm 4: No.05 code is realized according to the forward kinematics of left (right) arms of humanoid robot. No. 08 line code calculates the configuration increment and is realized according to increment equation (12) for inverse kinematics of left (right) arms based on SVD.

4 Computer 3d Simulation

Taking parallel grasping complex object by dual arm of humanoid robot in a multiple-obstacle environment, this paper has conducted a lot of computer 3D visualization simulation experimental verifications and researches on the proposed DAGRRT collision avoidance motion planning algorithm. Refer to Table 1 for D-H ($\theta_i, \alpha_i, a_i, d_i$) parameters for dual arm of humanoid robot. Left (right) arm has 7 rotating joints, the configuration space is $\mathbf{q}^k = [q_0^k, \dots, q_6^k]^T$ (k=R, L refer to left arm and right arm), each joint angle is randomly sampled within the scope of joint constraint. Open Inventor is adopted to construct 3D simulation scenarios including artificial dual arm, object and obstacle, and hierarchical bounding volumes algorithm for directions proposed by Gottschalk et al is applied to realize self-collision detection of dual arm of humanoid robot and scenario collision detection between humanoid robot and object or obstacle. Refer to Figure 4 for 3D display of planning outcome obtained from dual arm grasping object by DAGRRT algorithm, and 6 rectangle obstacles are randomly placed in the work space of humanoid robot. Subgraph (1) is initial configuration for dual arm, the initial configuration of left arm end effector is $(x, y, z, \phi, \theta, \psi) = (-729.387, 150.811, 1296.943, 1.669, 0.992, -2.542)$, and the initial configuration of right arm end effector is $(390.833, 138.736, 1320.031, -1.214, 1.048, 0.587)$. Subgraphs (2) and (3) are the middle grasping configurations of dual arm. Subgraph (4) is the grasping target configuration obtained from planning. The target configuration of left arm end effector is $(-204.765, 516.069, 1302.585, -0.150, -0.952, -2.499)$, and the target configuration of right arm end effector is $(207.720, 416.536, 1146.943, -1.874, 0.587, 0.317)$. Fig.5 is a 3D dynamic process of DAGRRT planning observed

from different perspectives. Figure 6 is 3D effect for simultaneously displaying RRT path and grasping set. Figure 7 is tracks after smoothness optimizing process of dual arm configuration obtained from DAGRRT algorithm. It can be seen from simulation outcome that the algorithm proposed in this paper can realize in parallel the operation task of collision avoidance motion planning of dual arm grasping object of humanoid robot accurately, effectively and efficiently in a complex obstacle environment.

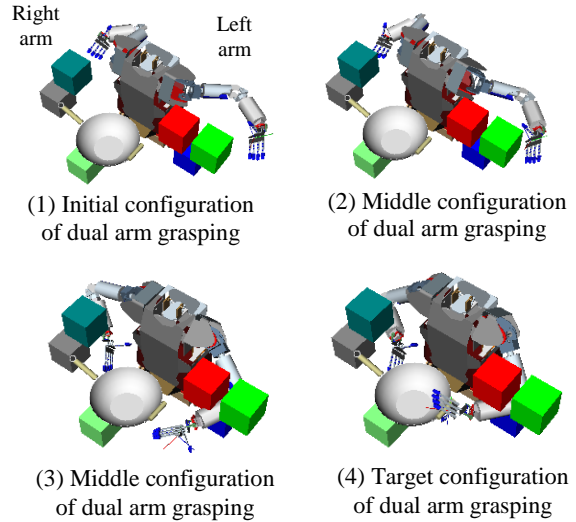


FIGURE 4 3D display of DAGRRT planning results

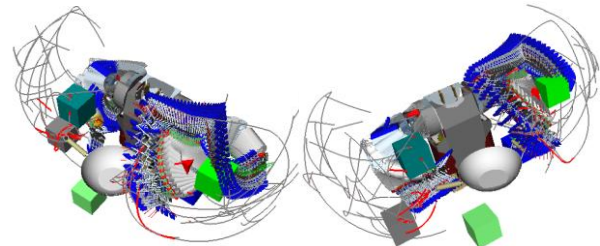


FIGURE 5 3D dynamic process of DAGRRT planning

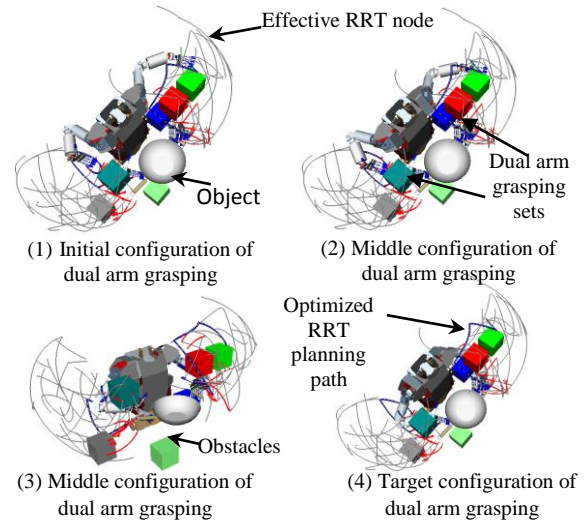


FIGURE 6 3D effect for simultaneously displaying RRT path and grasping set

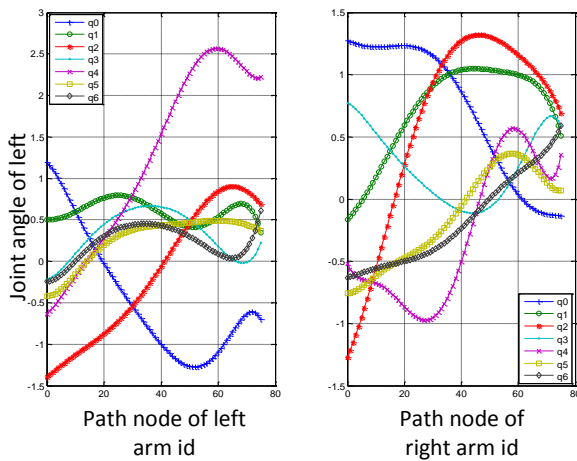


Figure 7 Tracks after smoothness optimizing process of dual arm configuration

TABLE 1 D-H parameters for dual arm of humanoid robot

Joint Variables	Theta (rad)	Alpha (rad)	a (mm)	d (mm)	joint constraint (rad)
q_0^L	$\pi/2$	$\pi/2$	0	0	$[-\pi/2, \pi/2]$
q_1^L	$\pi/2$	$\pi/2$	0	0	$[-\pi/2, \pi/2]$
q_2^L	$-\pi/2$	$\pi/2$	20	-310	$[-23\pi/18, \pi/2]$
q_3^L	0	$-\pi/2$	0	-7.5	$[-23\pi/18, \pi/2]$
q_4^L	$\pi/2$	$-\pi/2$	0	-240	$[-\pi, \pi]$
q_5^L	$-\pi/2$	$-\pi/2$	0	0	$[-\pi/2, \pi/2]$
q_6^L	$-\pi/2$	$\pi/2$	0	0	$[-\pi/2, \pi/2]$
q_0^R	0	$-\pi/2$	0	0	$[-\pi/2, \pi/2]$
q_1^R	$-\pi/2$	$-\pi/2$	0	0	$[-\pi/2, \pi/2]$
q_2^R	$\pi/2$	$\pi/2$	20	-310	$[-23\pi/18, \pi/2]$
q_3^R	0	$-\pi/2$	0	7.5	$[-23\pi/18, \pi/2]$
q_4^R	0	$\pi/2$	0	-240	$[-\pi, \pi]$
q_5^R	$\pi/2$	$-\pi/2$	0	0	$[-\pi/2, \pi/2]$
q_6^R	0	$\pi/2$	0	0	$[-\pi/2, \pi/2]$

Reference

[1] KE Wen-De, CUI Gang, HONG Bing-Rong, CAI Ze-Su, PIAO Song-Hao, ZHONG Qiu-Bo. Falling forward of humanoid robot based on similarity with parametric optimum. ACTA AUTOMATICA SINICA 2011 37(8): 1006-1012

[2] KE Wen-De, PENG Zhi-ping, CAI Ze-Su, CHEN Ke. Research progress on similarity locomotion of humanoid robot Application Research of Computers 2013 30(9) 2570-2575

[3] E. Yoshida, I. Belousov, C. Esteves, and J.-P. Laumond. Humanoid motion planning for dynamic tasks: Proceedings of the IEEE International Conference on Mechatronics & Automation, 2005. Niagara Falls, Canada July 2005 1784-1789

[4] L. Sentis and O. Khatib. Whole-body control framework for humanoids operating in human environments. Proceedings of International Conference on Robotics and Automation 2006 2006 2641-2648

[5] E. Drumwright and V. Ng-Thow-Hing. Toward interactive reaching in

5 Conclusion

Grasping operation of dual arm collision avoidance of humanoid robot is a critical technique involved in the motion planning research of humanoid robot. Aiming at such problems as grasping space limitation, redundancy constraint and unknown target configuration, this paper has put forward a dual arm grasping motion planning DAGRRT framework integrating SVD and RRT techniques and the realization of parallel processing algorithm. On the one hand, it makes full use of rapidly-exploring random tree (RRT) to seek completeness characteristic of the path; on the other hand, it uses singular value decomposition (SVD) to seek configuration singularity, meet inverse kinematics of dual arm in joint constraint, lead the dual arm of humanoid robot to parallel and expand from initial configuration to target object, find a collision avoidance path and complete the object grasping by dual arm. This method is of universal significance to simultaneous grasping by dual arm or control operation of humanoid robot for dynamic target or unknown target position in a complex environment.

Acknowledgements

This work was supported in part by a grant from Harbin Institute of Technology Robotics and System National Key Laboratory (SKLRS-2012-MS-06), Shenzhen Science and Technology Program (JC201006020820A and JCYJ20120615101640639), Team of Scientific and Technological Innovation of Shenzhen Institute of Information Technology (CXTD2-002), Natural Science Foundation of Guangdong Province, China (S2013010013779 and S2011040000672), Guangdong Vocational Education Information Technology Fund (XXJS-2013-1019).

static environments for humanoid robots. In IEEE/RSJ International Conference On Intelligent Robots and Systems (IROS), 2006. Beijing, China, Oct 2006 846-851

[6] H.-L. Cheng, D. Hsu, J.-C. Latombe, G. S'anchez-Ante. Multi-level free-space dilation for sampling narrow passages in PRM planning. In Proc. IEEE Int. Conf. on Robotics & Automation 2006 1255-1260

[7] ZHONG Qiu-Bo. Research on key technologies of motion planning for humanoid robot. Harbin: Harbin Institute of Technology 2011

[8] Ky Wen-De, Peng Zhi ping, Hong Bing rong, Xu Xian dong Locomotion similarity-based humanoid robot's stepping upstairs. J. Huazhong Univ. of Sci. & Tech. (Natural Science Edition) 2012 40(12) 60-64

[9] Wang Jian. Study on Humanoid online motion planning. Changsha :Graduate School of National University of Defense Technology 2008.

[10] LIAO Yi-huan, LU Dao-kui, TANG Guo-jin. Motion planning of space manipulator system based on a hybrid programming strategy. Journal

- of Astronautics 2011 32(1) 98-103
- [11] L. Jaillet and T. Siméon. A PRM-based motion planner for dynamically changing environments. In Proceedings of IEEE/RSJ International Conference on Intelligent Robots and Systems, 2004. Sendai, Japan, 2004 1606-1611
- [12] Z. Sun, D. Hsu, T. Jiang, H. Kurniawati, and J. H. Reif. Narrow passage sampling for probabilistic roadmap planning. IEEE Transactions on Robotics and Automation 2005 21(6) 1105-1115
- [13] K.I. Tsianos, I.A. Şucan, and L.E. Kavraki. Sampling-based robot motion planning: Towards realistic applications. Computer Science Review 2007 1(1) 2-11
- [14] Fu Genping. Research on gait planning and walking control for humanoid robot. Guangzhou: Guangdong University of Technology, 2013
- [15] Zhang Tong. Research on walking control and path planning of a humanoid robot. Guangzhou: South China University of Technology, 2010
- [16] S La Valle, J Kuffner. Rapidly-exploring random trees: Progress and Prospects. Proceedings of Algorithmic and Computational Robotics: New Directions, 2001 293-308
- [17] EGE E S. A new approach to increase performance of rapidly - exploring random trees (RRT) in mobile robotics. Proceedings of the IEEE International Conference on Robotics and Automation, April 17-19, 2006. Antalya. IEEE, 2006 851-855
- [18] KANG Liang, ZHAO Chun-Xia and GUO Jian-Hui. Improved path planning based on rapidly-exploring random tree for mobile robot in unknown environment. PR & AI 2009 22(3) 337-343
- [19] WANG Wei, LI Yan. RRT-based manipulation planning method for both arms of virtual human. Journal of System Simulation, 2009, 21(20) 6515-6518
- [20] LI Huazho, LIANG Yongsheng, DAN Tangren, ZHENG Hongying, WU Xianfeng. Collision-free Motion Planning Algorithm Based on RRT for Robot. Journal of Shenzhen Institute of Information Technology 2012 10(3) 20-27
- [21] LI Huazhong, LIANG Yongsheng, WANG Meini, Dan Tangren. Design and implementation of improved RRT algorithm for collision free motion planning of high-dimensional robot in complex environment. ICCSNT 2012, 2nd Int. Conference on Computer Science and Network Technology 1391-1397
- [22] J.J. Kuffner, K. Nishiwaki, S. Kagami, M. Inaba, and H. Inoue. Motion planning for humanoid robots. In Proceedings of 11th International Symposium of Robotics Research, 2003. 2003:365-374.
- [23] J.J. Kuffner, S. Kagami, K. Nishiwaki, M. Inaba, and H. Inoue. Dynamically stable motion planning for humanoid robots. Autonomous Robots 2002 12(1) 105-118
- [24] Wang Wei. Key technical research on motion planning and motion synthesis for virtual human. Changsha: Graduate school of national university of defense technology 2011
- [25] D. Bertram, J.J. Kuffner, R. Dillmann and T. Asfour. An integrated approach to inverse kinematics and path planning for redundant manipulators. In Proceedings of IEEE International Conference on Robotics and Automation 2006 1874-1879
- [26] M.K. Weghe, D. Ferguson, and S.S. Srinivasa. Randomized path planning for redundant manipulators without inverse kinematics. In Proceedings of IEEE International Conference on Humanoid Robots 2007 477-482
- [27] D. Berenson, S.S. Srinivasa, D. Ferguson, J.J. Kuffner. Manipulation planning on constraint manifolds. In Proceedings of IEEE International Conference on Robotics and Automation, 2009. 2009:625-632.
- [28] L. Guilamo, J. Kuffner, K. Nishiwaki, S. Kagami. Efficient prioritized inverse kinematic solutions for redundant manipulators. IEEE/RSJ International Conference on Intelligent Robots and Systems 2005 3921-3926
- [29] HAN Zheng, LIU Huaping, HUANG Wenbing, SUN Fuchun, GAO Meng. Kinect- based object grasping by manipulator. CAAI Transactions on Intelligent Systems 2013 8(2) 149-155
- [30] Yang Ben. Research on motion control of a 7-DOF manipulator. Han zhou: China jiliang university 2012
- [31] WANG Xiao-ping, DONG Xiu-cheng. The solution to collision detection of moving object simulation. Journal of Xihua University Natural Science 2013 32(5) 15-17
- [32] XIE Shi-fu, MA Li-yuan, LIU Peng-yuan, MA Long. Research and realization of collision detection algorithm for dynamic cable in virtual environment. Journal of System Simulation 2013 25(8) 1865-1870
- [33] JIANG Xiaolu, LIU Yuan. New collision detection algorithm based on hybrid hierarchical bounding box. Computer Engineering and Applications 2012 48(6) 143-145
- [34] S.Gottschalk, M.C.Lin, D.Manocha. OBBTree: A Hierarchical structure for rapid interface detection. Proc. of SIGGRAPH'96. 1996 171-180

Authors	
	<p>Li Hua-zhong, 1963</p> <p>Current position, grades: Ph.D., associate professor Scientific interests: intelligent robots, space robot, virtual reality, path planning.</p>
	<p>Liang Yong-sheng, born in July, 1971</p> <p>Current position, grades: Professor University studies: Harbin Institute of Technology Scientific interest: Information and Communication Engineering</p>
	<p>Tang Qiang-ping, born in 1960, Zhejiang, P.R. China</p> <p>Current position, grades: Professor University studies: Northwestern Polytechnical University Scientific interest: Computer applications</p>